Korean J. Chem. Eng., 39(8), 2099-2108 (2022)
DOI: 10.1007/s11814-022-1130-3

pISSN: 0256-1115
eISSN: 1975-7220

An experimental study on polymer cathode materials in lead-acid battery energy storage systems

Davoud Jahani*,†, Amin Nazari, Mohammadreza Yazdan Panah***, Nader Javani****, and Fatemeh Moharaminezhad*****

*Department of Mechanical Engineering, Faculty of Engineering, University of Bonab, Bonab, Iran
**Department of Chemical Engineering, Faculty of Engineering, University of Maragheh, Maragheh, Iran
***Department of Chemical Engineering, Faculty of Engineering, University of Bonab, Bonab, Iran
****Faculty of Mechanical Engineering, Yildiz Technical University, 34349, Istanbul, Turkey
*****Faculty of Nanophysics, Kashan University, Kashan, Iran
(*Received 25 December 2021 • Revised 14 March 2022 • Acceptedc 2 April 2022*)

Abstract−The replacement of lead grids with acrylonitrile butadiene styrene (ABS) polymer grids in the negative electrode of lead-acid batteries was studied experimentally, while the positive electrode remained unchanged. A polymer grid was activated by nickel plating using a chemical solution, and then coated with chrome and copper conductive plating. The polymer grid was coated with a layer of lead. Using a lead-coated polymer grid, a 30-amp 12-volt battery was produced and tested, and the results were compared with a 30-hour production line lead-acid battery. The results show that the polymer grid has a strong ability to generate an appropriate voltage in the charge and discharge cycle and create a stable capacity. The results also show the polymer grid weight has decreased significantly (about 50%) compared to the conventional lead grid. In this work, the adhesion of a negative paste to the surface of the polymer grid covered with the lead-exposed expand grid was studied, and the results show that the polymer grid can adhere to the negative dough perfectly.

Keywords: Energy Storage, Lead Acid Batteries, Abs Polymer, Electrode, Polymer Grid

INTRODUCTION

Many researchers aim to develop different techniques to increase the energy density and power density of batteries [1]. The operational principles and fundamentals of lead-acid batteries have been discussed in detail among the researchers, before the widespread use of other battery types [2]. Industrial projects such as Melt-spun and sintered Metal fibre networks for lead-acid batteries (MEMLAB) were carried out to increase the energy density of the battery. Titanium metal fibers are used with a density of 4.5 g/cm^3, and there was a significant reduction in the weight of the grids [3,4]. In recent years, Li-ion batteries have manifested a much higher power density and, therefore, they are used in many applications. For lithium-ion batteries, limited lithium sources and low safety associated with flammable organic electrolytes significantly hinder their large-scale application [5,6]. Effective thermal management systems must be employed in Li-ion batteries. There are active and passive cooling systems for this purpose. Recent studies try to use the passive phase change materials for thermal management of batteries as separate [7] or integrated into battery modules [8].

Aluminum-ion rechargeable batteries (AAIBs) have attracted much attention due to their high theoretical capacity, high volumetric energy density, and low price [9,10]. However, due to the low standard reduction potential of Al^{3+}, not many aqueous full batteries have been developed successfully [11,12]. He et al. [13] demonstrated a rechargeable aqueous Al-S battery based on a water-in-salt electrolyte with the configuration of Al, $Al(OTF)_3$+LiTFSI+HCl, S/C. While aluminium, lithium, graphite, and vanadium batteries are the new generations of rechargeable batteries [14,15], lead-acid batteries are steadfast, tried-and-true market leaders, with a global market of $58.5 billion [16]. The reason why hybrid electric vehicle (EV) automakers choose to use the lead-acid battery for the starting, lighting, and ignition (SLI) functions is due to affecting parameters such as their safety and cost [17,18].

The first lead-acid battery, the oldest rechargeable battery, was invented in 1859 by Raymond Gaston Plante, a French physicist. After 160 years still, lead-acid batteries are found in cars, scooters, wheelchairs, UPS systems, etc. Lead-acid batteries are more dependable, economical, and environmentally sustainable than their competitors [19,20]. The Advanced Lead Acid Battery Consortium (ALABC) has been working on the development and promotion of lead-based batteries for sustainable markets such as hybrid electric vehicles (HEV), start-stop automotive systems, and grid-scale energy storage applications. Considering fossil fuels' effects on the environment and their limitation on accessibility, rechargeable lead-acid batteries are considered as one of the most reliable energy storage systems and many researchers are studying the different aspects of these products [21]. One of the reasons for the acceptance of lead-acid batteries is their operating flexibility in different temperatures. One main issue of lead-acid batteries, which is the main focus

†To whom correspondence should be addressed.
E-mail: davoud@ubonab.ac.ir

of the current study, is their chemistry. The sulfation of negative plates should be prevented. Gao et al. [22] proposed a novel Pb/PbO@C nanocomposite sharing a 3D conductive carbon network with macropores, derived from eggplant biomass to improve the lifespan of lead-acid batteries (LABs) and to overcome the irreversible sulfation. This effectively facilitates electron transport and boosts ion diffusion as well as suppresses the growth of $PbSO_4$ during the charge-discharge process. In lead-acid batteries, by increasing discharge current and discharge depth, the reversibility of lead-carbon batteries becomes worse and worse. Li et al. [23] synthesized an NSCG@PbO nano-lead oxide and multifunctional porous carbon on graphene framework by sol-gel pyrolysis, which restricts the formation of large particle $PbSO_4$, effectively increases the porosity of lead-carbon electrode, maintains the electrochemically active surface area of the lead-carbon battery. Lead-acid batteries are commonly associated with relatively heavy lead grids and active materials and, consequently, less specific energy [24]. Lightweight products have always been important in product designs across several industries. Reducing the weight of the batteries by grid weight reduction to improve specific energy of the batteries has been the subject of many research works [25,26]. The grid has two functions in the acid lead battery: current collector and active material backup. Lead does not participate in the electrochemical reaction in the lead electrode grid, but only provides the necessary strength and rigidity for the grid to withstand environmental pressures and the manufacturing process. To reduce the total weight of an acidic lead battery, reducing the weight of the grid forming the electrode is an effective method. Zhang et al. designed a novel polymer-graphite composite grid as the negative current collector for lead-acid batteries [27]. They conducted structural optimization and surface treatment on the grid to improve its performance. Through structural optimization, additional lead pastes were loaded and the cycle stability of the battery was enhanced. Using the optimized grid, the weight of the negative current collector was reduced by more than 50%. To handle the serious hydrogen evolution on the graphite surface and the unfavorable adhesion between graphite and NAM, fine $PbSO_4$ particles were coated onto the surface of the graphite grids by chemical deposition. The cells employing the $PbSO_4$-deposition grids exhibit excellent cycling stability and low polarization and then high Coulombic efficiency. Soria [28], with the final goal of increasing the energy density utilizing a battery weight reduction, substituted the heavy lead alloy grids (mechanical support of the active masses and collectors of the current produced during the charge and discharge reactions) with lightweight metallized polymeric network structures (PNS) with reduced mesh dimensions in comparison to conventional grids. The network was then coated with conductive materials and corrosion-resistant layers to conduct current flow. The electrode characteristics and the design features of the batteries prepared in the project were described, and their electrical performance was studied. Toniazzo proposed a new high-performance polymeric separator for lead-acid batteries [29]. Polymeric calendared ribbed separators are traditionally used in gel VRLA batteries. For this technology, the separator is required to have high pore volume, optimized pore size, low acid displacement, and low electrical resistance. It must also support efficient and controlled oxygen transfer. Glass-microfiber separators are presently the preferred material for AGM batteries. In addition to the properties listed for the polymeric type, glass-microfiber separators must not allow any drainage or stratification of the liquid electrolyte, and they can retain their initial thickness after filling and during the battery life to sustain the initial compression in each cell. The Amersorb separator is well adapted to both technologies, for example: (i) the ribbed and corrugated patterns provide improved porosity (pore volume and pore-size distribution); (ii) the flat membrane is not only able to wick and retain acid, but also has optimal compression properties (low compressibility and excellent springiness). Kirchev [30] proposed carbon honeycomb grids for lead-acid batteries. The carbon honeycomb grid is proposed as an innovative solution for high-energy-density lead-acid batteries. The proof of concept is demonstrated, developing grids suitable for the small capacity, scale of valve-regulated lead-acid batteries with 2.5-3 Ah plates. The manufacturing of the grids includes fast, known and simple processes that can be rescaled for mass production with minimum investment costs. The most critical process of green composite carbonization by heating in an inert, atmosphere from 200 to 1,000 °C takes about five hours, guaranteeing the low cost of the grids. An AGM-VRLA, cell with a prototype positive plate based on the lead-2% tin electroplated carbon honeycomb grid and, conventional negative plates is cycled, demonstrating 191 deep cycles. The impedance spectroscopy, measurements indicate the grid performance remains acceptable despite the evolution of the corrosion, processes during the cycling. Thin films of nanostructured lead dioxide were investigated as a positive electrode material for a lightweight lead-acid battery [31]. Martha [32] prepared lightweight grids for lead-acid battery grids from acrylonitrile butadiene styrene (ABS) copolymer followed by coating with lead. Subsequently, the grids were electrochemically coated with a conductive and corrosion-resistant layer of polyaniline. The specific energy of such a lead-acid battery was about 50 Wh/kg. Their developed batteries would withstand fast charge-discharge duty cycles.

Lim [33] developed a SnO_2 anode with a bimodal porous, fabricated using a randomly packed silica template with Sn precursor. They produced bimodal porous electrodes with SnO_2 nanoparticles to achieve controlled pore structures for alleviating the issue of volume change. Asif et al. [34] synthesized SnO_2-rGO composites at low temperatures and tested them as cathodes for Mg batteries. Their developed Mg batteries showed considerable specific capacities and capacity retentions.

Pinsky et al. [35] patented a battery with a tin oxide-coated grid. Their developed grid bed was made of fibreglass, covered with a tin oxide coating, making it electrically conductive. Their production capacity in the produced grid was reported to be stable due to the high stability of their developed structure in an acidic environment. However, they used glass fiber substrate, which is much more expensive than polymer. Furthermore, in their work, unlike our study, an industrial-scale battery was not developed. Shivashankar et al. [36] studied to reduce the weight of lead-acid batteries by using grids with lighter substrates. Their grids were made of an alloy of aluminum, and titanium, and a layer of 20 μm lead alloy coating on the grids to prevent corrosion in an acidic environment. Their material selection caused considerable weight reduction in the produced battery. In this study, grids made of ABS were used

to reduce the weight of a lead-acid battery significantly.

The goal of this study is to introduce an industry-level ABS for lead-acid batteries, which is economically accessible. Compared to the other polymers, ABS shows promising properties for plating due to its good moldability and flexibility, low production cost, high adhesion, good appearance quality, dimensional stability, and easy production. ABS softens at 100 °C, and it is obtained from the polymerization of three materials, acrylonitrile, butadiene, and styrene. These rubber particles make this material resilient. These particles corrode in contact with chemical solutions and create cavities in the polymer that improves the adhesion of the plated metal layer to the plastic. The main goal of this research work was to study the possibility of significant weight reduction of a lead-acid battery without considerable change in its power. Material change of one of the grids was suggested and studied in the research work. In this study, the replacement of lead grid with ABS polymer grid in the negative electrode of acid lead batteries while the positive electrode remained unchanged is studied experimentally. ABS polymer grids varying in size and thickness were prepared using a 3D printer. The polymer grids are activated by nickel plating using a chemical solution, and then coated with chrome and copper conductive plating. Finally, the polymer grid is coated with a layer of lead. Using a lead-coated polymer grid, a 30-amp 12-volt battery was produced and tested, and the results were compared with a 30-hour production line lead-acid battery. Capacity results showed that the ABS grid suggested battery can generate capacity and keep the potential difference constant in different cycles. The results showed that the polymer grid could conduct electrical conduction and generate the appropriate voltage in the charge and discharge cycle and create a stable capacity.

EXPERIMENTAL STUDY

1. Materials and Methods

Polymer grids were manufactured using acrylonitrile butadiene styrene (ABS) filaments and a 3D printer, as shown in Fig. 1. ABS, like other polymers, is non-conductive, and it is not possible to make copper or different kinds of plating. Manufactured ABS grids were processed in several steps, as shown in Table 1, before copper plating.

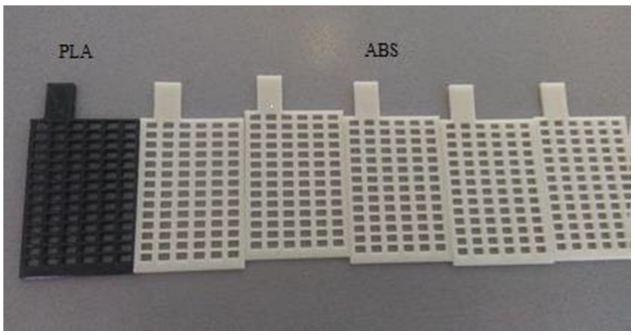

Fig. 1. Printed network of ABS batteries.

Copper plating was performed on the produced ABS grids after the process in Table 1 was achieved. Later, they also were covered with a lead layer. Fig. 2 shows ABS grids after copper and lead plating. Scanning electron microscopy was used to determine the thickness of the plated layers on the polymer grid.

The plated polymer grids were tested by single-plate testing after the completion of the manufacturing process to assess the capacity in the charging and discharging function and create a stable potential difference in the negative plates. The specifications of a battery produced by developed polymer grids, a battery taken from a typical lead-acid battery production line, were compared. The curing process of the negative plates was carried out at 60 °C and humidity of 90%. This process took place 48 hours, using an automotive curing machine. After complete formulation of the plates, the capacity test was covered as a single plate on the negative plates with a polymer grid and the negative plates of the line were performed as a control sample. The weight of the polymer grid with a lead flag is 16 grams, and the weight of the routine expands network is 36 grams. Then, the lead flag was used to make the plate category in

Table 1. ABS grid processing steps

Step number	Procedure name	Used materials	Procedure temperature range (°C)	Processing time (minutes)
1	Cleaning	Trisodium phosphate 120 (mg/liter) Sodium carbonate 15 (g/liter) Oleic acid 15 (g/liter)	50-60	2
2	Acid washing	Acid Sulfuric 50 (cc/liter) Chromic acid 400(g/liter)	50-60	2-5
3	Etching	Acid Sulfuric 1.80 (cc/liter) Chromic acid 430 (g/liter) Phosphoric acid 30 (g/liter)	50-60	2-3
4	Neutralization	Acid chloric 180 (cc/liter)	40	1-2
5	Sensitization	Tin chloride 125 (g/liter) Palladium 0.25 (g/liter) Chloric acid 20 (cc/liter)	35-40	5-10
6	Accelerating	Chromic acid 400 (g/liter)	20-50	At least 2

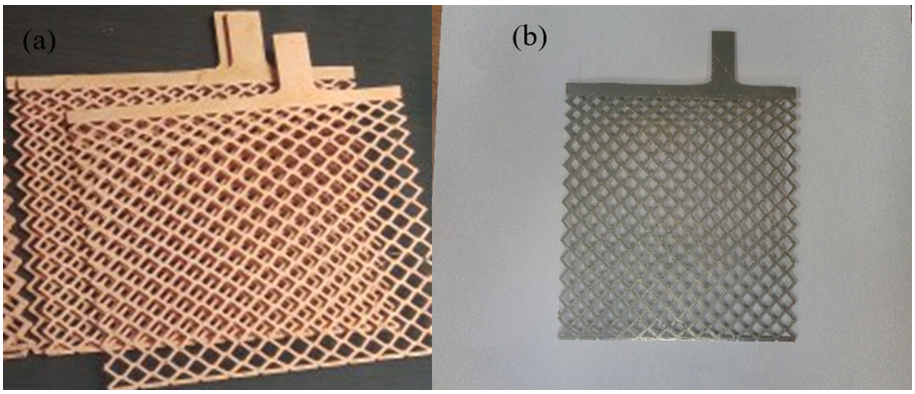

Fig. 2. (a) Copper coated polymer grid, (b) Lead coated polymer grid.

Table 2. 30 Amp battery formulation program

The level	Amps	Time
First stage	6 amps	19.20 minutes
Second stage	Zero amp	10 minutes
Third stage	3.27 amps	0.5 hours

Table 3. Characteristics of polymer plating with a thickness of 1 mm for single plate testing

Grid type	Grid weight with flag	Grid weight with dough
Expand ABS	17.21	102.21
Expand ABS	17.75	102.75
Expand ABS	16.35	102.58
Expand ABS	17.04	100.85
Expand ABS	18.44	103.44
Expand ABS	19.56	104.56

the polymer grid. To make a 30 amp 12-volt battery, a lead-coated polymer-expand grid was used as a negative electrode, and a positive-excited lead-positive grid was used as a positive electrode with a negative 3-page and 3-positive arrangement. For the process of forming or pre-charging the 30 amp battery, first, all the battery cells were filled with sulfuric acid with a density of 1.24 g/cm^3, and then the battery was charged according to Table 2 [3,37,38].

Expanded polymer plating was plated with 72 g of negative dough. Expand-free lead mesh no dough weighs 36 grams and plated ABS polymer plating weighs 20.8 grams. It is worth mentioning the grid flag was a lead polymer, and the plating thickness was 2 mm. The negative dough used was 85 g, and the reason for the weight change was due to the variable weight of the solder that was reported to connect the lead flag to the grid in Table 3.

2. Fundamentals of a Bipolar Configuration

Power output is the most significant advantage of a battery with a bipolar configuration over the conventional monopolar configuration. In a conventional battery, electrons generated because of electrochemical reactions travel from active materials to a current collector (i.e., grid) and subsequently to the next cell through an outer circuit element. However, in bipolar batteries, electrons directly travel to the next cell through the substrate (partition wall) as positive and negative active materials are placed on the two opposite faces of a bipolar substrate (Fig. 3). Lead metal improves the soldering properties of the polymer mesh, so for better soldering, a lead coating was created by plating the mesh surface. The role of grids is to store active materials and to establish an electrical connection between the active materials and the battery poles. The preparation of electrode paste is a key step in preparing the active ingredient and determining the performance of lead-acid batteries. The paste must be able to flow under pressure in the lattice and remain on the lattice throughout the curing operation as well as in

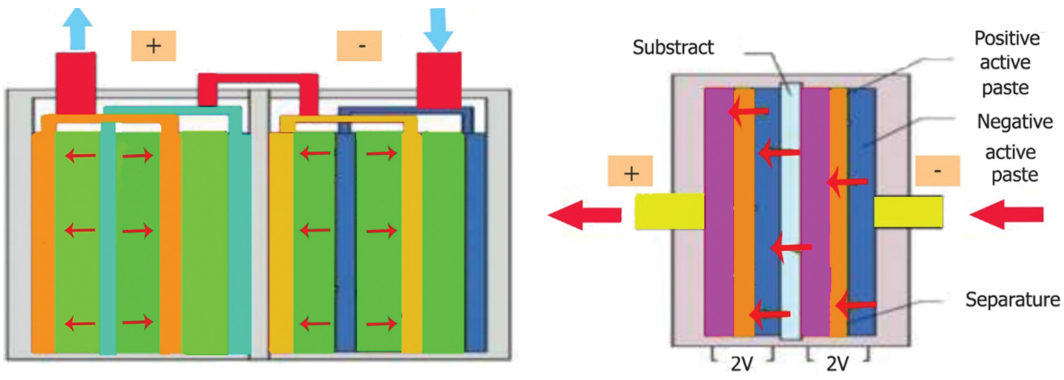

Fig. 3. Conduction path inside a lead-acid battery while charging; 4 V conventional monopolar (left) versus bipolar (right) design.

the drying process where the material requires hardness and cohesion between the particles. After curing the active ingredients must have a maximum of 2% lead and 1% moisture. At this stage the single crystals join together to form a strong structure with high porosity, the plates become rechargeable plates as they lose their water; during this stage, the metal head is wholly oxidized, and the amount in the paste is minimized. Sulfuric acid is a clear, oily, odorless, water-soluble liquid when the acid dissolves in water; it heats up violently, damaging leather, paper, and clothing, and is used as the electrolyte of lead-acid batteries. The next step is the process of charging the plates, which is an electrochemical operation during which the complete chemical conversion of the active ingredients takes place. In all batteries, insulation between the anodes and cathodes of each plate category is essential. In addition to preventing short-circuits of positive and negative electrodes, the separator acts as a barrier to the transfer of active material between the plates and reduces the loss of active material. A simple cell comprises a negative electrode, a positive electrode, and a division between them. In practice, most cells are made from 3 to 30 pages with a separator between them. The positive and negative plates prepared after the page charging operation are usually assembled in parallel groups or batches with an additional negative plate, and separators, holders, and spacers are placed between these plates.

3. Preparation of Plate Handles from Plates with Polymer Mesh to Evaluate their Performance

The ability to produce a set of galvanized polymer plating sheets in the COS process was investigated when the nets were placed inside the lead melt and the connection in the flag area was tested. The layout of the nets is used as one in the middle of 6 lead expands nets with positive paste and five expander polymer nets coated with lead or negative paste. This arrangement, like routine line batteries, can supply AH 55 capacity. After connecting the flags to perform the charge-discharge cycle and checking the capacity of the page handle, the page handle prepared inside the electrolyte was placed at a density of 1.24 and the formation process was performed. Then the capacity test took place with a discharge current of 2.75, shown in Fig. 4.

4. Preparation of 55 amps 12 volts Battery Using Negative Polymer Grids

Each cell in a 55 amp battery has five negative electrodes with a polymer grid covered with a head and six positive electrodes with a lead grid. Each battery contains six cells. Hence, 30 negative electrodes and 36 positive electrodes are located in a battery.

The average weight of negative electrodes with a polymer grid to make a 55 amp battery is 99.28 gr. Given that the weight of the

Table 4. Specifications of lead-coated polymer negative grid for 55 amp battery

Number	The weight of the negatively soldered grid	Negative electrode weight
1	23.53	101.53
2	21.97	99.97
3	23.10	101.1
4	22.31	100.31
5	21.30	99.33
6	22.79	100.79
7	25.40	103.40
8	23.39	101.39
9	22.21	100.21
10	22.93	100.93
11	24.86	102.86
12	19.04	97.04
13	24.59	102.59
14	25.34	103.34
15	21.12	96.04
16	22.18	100.18
17	16.97	94.97
18	21.12	99.12
19	18.52	96.52
20	16.31	94.31
21	17.62	95.62
22	18.04	96.04
23	20.67	98.67
24	20.78	98.78
25	21.72	99.72
26	16.90	94.9
27	23.17	101.17
28	23.14	101.14
29	21.75	99.75
30	18.80	96.8

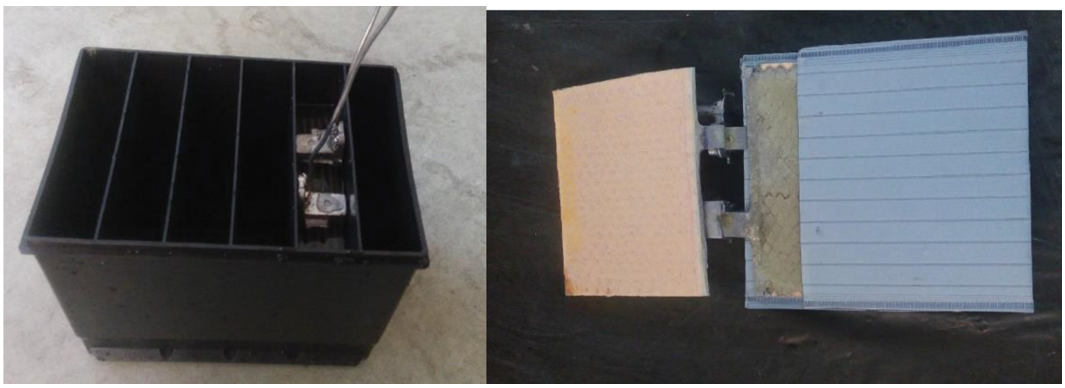

Fig. 4. Schematic of the page category after the process.

Table 5. 55 amp battery charging program

The level	Amps	Time
First stage	11 amps	19.20 minutes
Second stage	Zero amp	10 minutes
Third stage	6 amps	0.5 hours

plates produced with the lead plated used in the production line has an average weight of 114 gr, therefore, the weight of the negative electrode is reduced by 15 gr on average. The weight of a 55 amp-hour battery with a polymer-negative network has been reduced by about 450 gr compared to a battery with a lead-negative grid in Table 4. For the preparation of the batteries, first, all the battery houses were filled with sulfuric acid, 1.24 g/cm^3, and then the batteries were charged, as shown in Table 5.

After charging, the density of acid in each house reached 1.28 g/cm^3, and the final output voltage of the battery became 11.80 volts. The battery was tested for performance and compared with the battery produced with the lead grid. A battery is designed for 30 amps of 12 volts consisting of 6 two-volt cells. Each cell in the 30 amp battery has 3 negative electrodes with lead-plated and 3 positive electrodes. And, each battery has 6 cells, 18 negative electrodes and 18 positive electrodes. On average, the weight of negative plates with polymer plating and the lead plate is 94.97 and 114 gr, respectively. Weight and performance of 30 amp battery produced with a negative lead grid in total compared with the battery with the lead grid.

RESULTS AND DISCUSSION

1. Scanning Electron Microscopy Analysis (SEM)

Fig. 5 presents the SEM image of the electroplated lead on vitreous ABS. As it can be seen, four layers with a thickness of about two μm are created. The plated layers on the polymer mesh substrate are nickel, chromium, copper and lead. The thickness of the lead coating was about 10 μm, which agreed with the calculated thickness values of the lead layer on the base of Faraday's law. It can be seen from the images that the ABS is completely covered with lead coating and the electrodeposited lead has good contact with the ABS. The surface of the lead coating is also uniform over the whole surface. Results obtained for large ABS collectors are similar to those achieved for smaller ones. An SEM image from the plating layers on the surface of the polymer-coated grid is shown in Fig. 5. The thickness of the coating at the cross-sectional is also

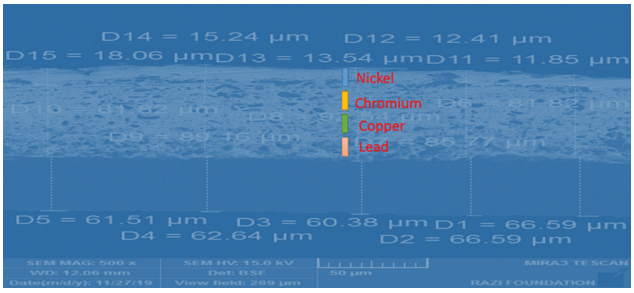

Fig. 5. SEM image, taken from the cross-sectional area of the polymer network.

Table 6. The thickness of plating layers

Layer material	Average coating thickness (μm)
Nickel	1
Chrome	65
Copper	88
Lead	14

given in Table 6.

The first layer is made of nickel on a polymer plating and is coated on the plating as the first layer with a thickness of one micrometer due to its low thickness. Plated layers on the substrate of the polymer network are nickel, chromium, copper and lead, respectively.

To compare the dough adhesion test to the grid on the plates with the polymeric and routine plates, the drop test was performed (Fig. 6 and Fig. 7). To perform the negative grid test, the gird is released from a height of one meter after the curing process. Repeating this procedure ten times and comparing the amount of negative dough adhesion in the grids through the amount of dough falling from the grid surface have been conducted. The results show the negative dough stickiness leads to an expanded grid (LAN line)

Fig. 6. Negative plate production line after the drop test.

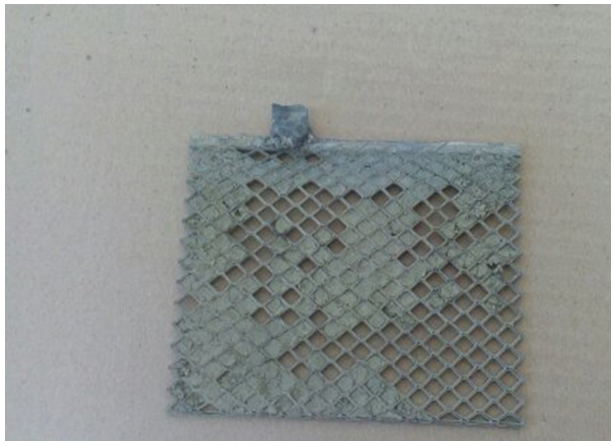

Fig. 7. Negative plate made of polymer-coated with the lead after drop test.

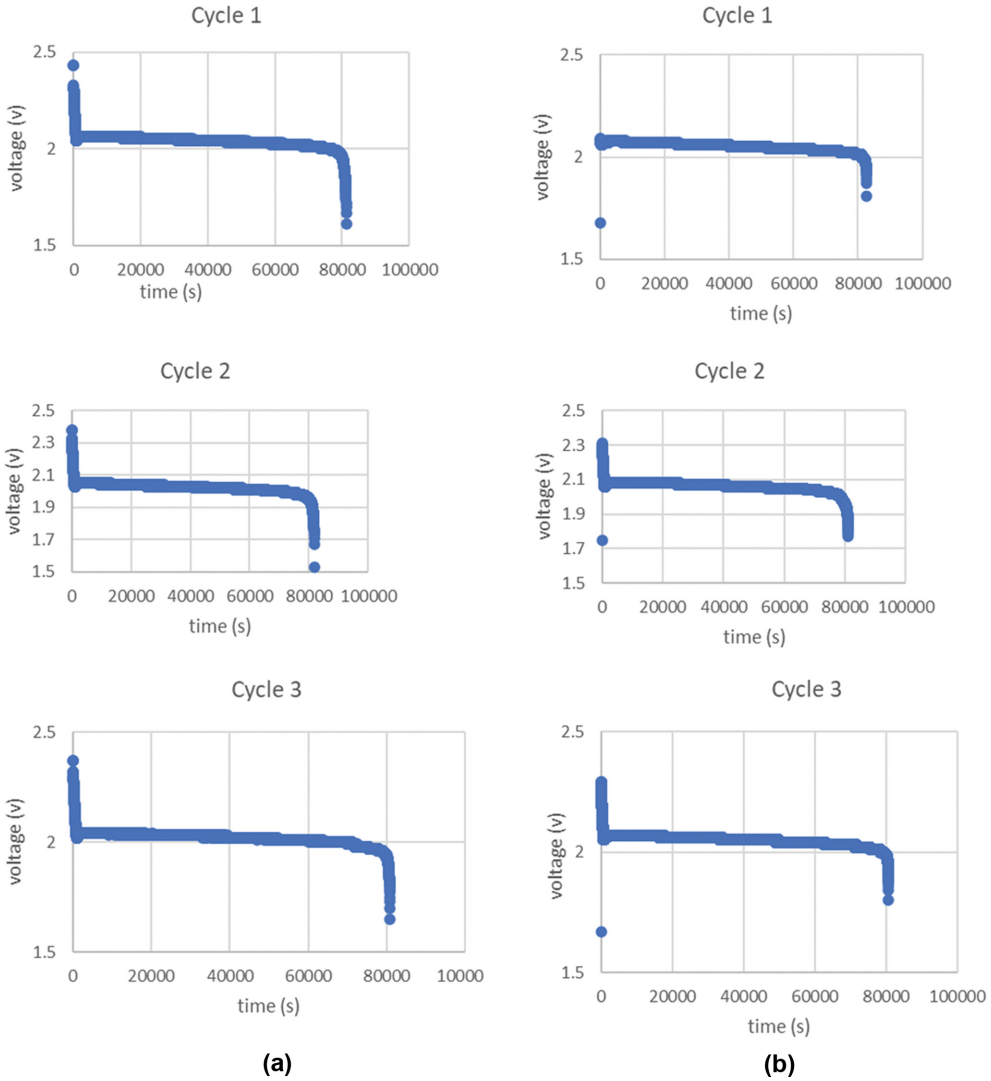

Fig. 8. (a) Discharge diagrams of expanded polymer grid with lead coating in single plate (b) discharge diagram of the lead expanded grid in a single plate.

higher and relatively less sticky dough roll is the expanded grid [4].

One of the main goals was to build a lightweight battery grid to replace the lead grid, which can generate capacity equal to the lead grid, having good electrical conductivity to collect electricity from electrochemical reactions and stability in acidic environments. Routine negative plates of line with negative polymer plates were tested as a single plate after the formation process to check the capacity and cycle of the discharge cycle with a current of 0.5 amps. The results of the discharge cycle diagrams in Fig. 8 show that this network can generate a constant potential difference in different cycles [39-41].

To calculate the capacity produced on the negative sides of the routine, lines were calculated with negative polymer plates and the obtained results are shown in Tables 7 and 8.

The result of this study show that in the developed batteries the active materials at the grid level are stable during different cycle operations. This is because the lead grid has good stability in an acidic environment and can collect the current produced by the electrochemical reaction. The lead-coated polymer grid was discharged at a current of 0.5 amps per hour. This grid can create a stable potential difference in different cycles, but the capacity produced is less compared to the lead grid. This is because active materials were removed from the surface of the grid. Lead expanded grid and expanded polymer grids in a single test plate are compared and shown in Fig. 9. Negative plates with plating grid can produce close capacities and could be introduced to grids as a viable alter-

Table 7. Capacity line routine negative plates in three successive cycles of charge and discharge (single plate)

Discharge cycles of the lead expanded grid	Capacity (Ah)	Discharge time (h)	The energy density (Ah/gr)
Cycle 1	11.4777	22.95	0.3188
Cycle 2	11.2636	22.52	0.3128
Cycle 3	11.1905	22.38	0.3108

Table 8. Capacity polymer negative plates in three successive cycles of charge and discharge (single plate)

Discharge cycles expanded grid of ABS/Lead	Capacity (Ah)	Discharge time (h)	The energy density (Ah/gr)
Cycle 1	11.287	22.57	0.5643
Cycle 2	11.355	22.71	0.5677
Cycle 3	11.229	22.45	0.5708

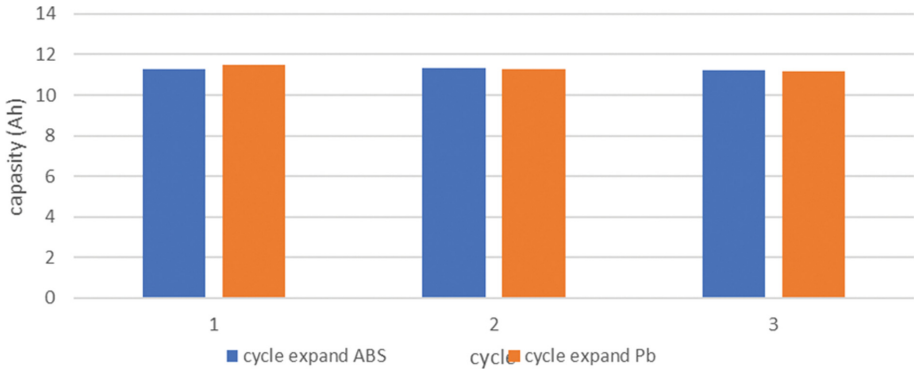

Fig. 9. Capacity comparison of expanded ABS and lead grids.

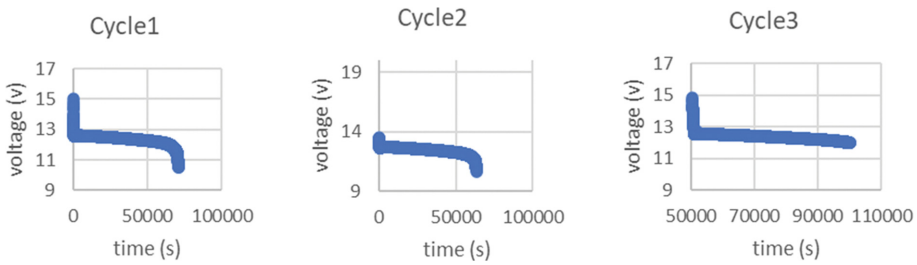

Fig. 10. The first cycle curve of 30 amp battery discharge at 12 volts in the production line.

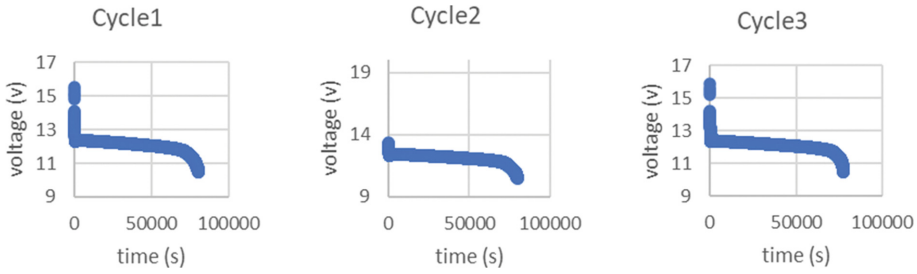

Fig. 11. The first cycle curve of 30 amp battery discharge at 12 volts contains negative polymer plates.

native to lead-acid batteries in the construction of the batteries.

Comparing the discharge curves in a battery with a negative polymer grid covered with lead and a battery with a lead network are shown in Fig. 10 and 11. A 30 amp 12-volt battery can generate a constant potential difference over time and store about 30 amps of energy.

Charging and discharging results for the adhesion of a negative paste to the surface of the polymer grid, the results of a battery of 30 ampere-hours capacity of the first to third line routine with plates and 30 ampere-hour battery provided with a negative network expanded polymer are listed in Tables 9, 10, and 11, respectively.

The average capacity of the first to third batteries prepared from the negative polymer grid is 27 amps. The average first to the third capacity for a battery with linear routines is 33 amps.

According to Iran's national standard, the cold start was performed at minus 18 °C. In 30 Amp batteries made with led expand and lead-coated polymer grids, the cold start test was performed and compared (Fig. 12). Both batteries were discharged for 30 seconds with a current of 6 volts at 190 amps, followed by a break of 20 seconds with 114 amps. In both batteries, a very small voltage drop occurred. The battery voltage of 30 amps with routine lines is 8.2 volts at the end of ten seconds, while for a battery-powered by a

Table 9. Charging and discharging results for the adhesion of a negative paste to the surface of the polymer grid

Discharge cycle	Capacity (Ah)	Discharge time (h)	Density (Ah/gr)
Cycle 1	3.428	6.84	1.1412
Cycle 2	3.7906	7.58	1.2635
Cycle 3	3.8795	7.75	1.2931
Cycle 4	3.8851	7.75	1.2950
Cycle 5	3.9268	7.85	1.3089
Cycle 6	3.8643	7.72	1.2881
Cycle 7	3.7490	7.49	1.2496
Cycle 8	3.7198	7.43	1.2399
Cycle 9	3.6031	7.20	1.2010

Table 10. The battery capacity of 30 amps at 12 volts with negative polymer plates in successive charging and discharging cycles

Discharge cycle	Capacity (Ah)	Discharge time (h)
Cycle 1	29.59	19.72
Cycle 2	26.35	17.56
Cycle 3	24.99	16.66

Table 11. Battery capacity 30 amps 12 V production line in successive charging and discharging cycles

Discharge cycle	Capacity (Ah)	Discharge time (h)
Cycle 1	33.6	22.4
Cycle 2	33.31	22.21
Cycle 3	32.30	21.53

negative polymer network it is 6 volts. The potential drop for the polymer network battery is greater in the first ten seconds [5,42,43].

The battery provided by the lead line of the performance line has a better effect on the start test in the cold. This is due to the low thickness of the plated lead layer. Due to the low thickness of the plated lead layer on the polymer grid, it is less possible to discharge with high currents in the polymer battery. To perform the battery charge test, it was discharged at 25 C for 5 hours. Current I. is calculated based on Eq. (1).

$$1=\frac{C_e}{10} \quad (1)$$

After discharge, the battery should be placed in a refrigerator until its temperature reaches 0 °C and then kept at this temperature for 20 hours. The battery is then quickly removed from the refrigerator and charged at a constant voltage of 14.4 volts, and after 10

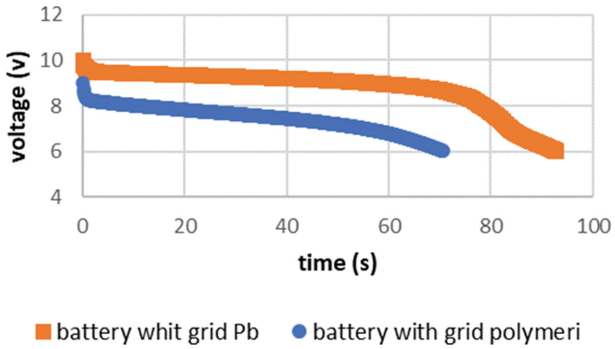

Fig. 12. Voltage diagram in terms of time to determine the time to reach the voltage of 6 volts in the cold start test.

minutes from the start of charging, the charging current is recorded. This current was recorded as a charging current. The result shows that batteries produced with polymer networks have the same charging capability as the routine networks, as presented in Table 12 [44,45].

The acceptance results for a 30 amp-hour battery with linear routine plates and a 30 amp battery with a negative polymer grid are 2.8 and 2.5, respectively. The slight difference (about 0.3) for the charging acceptance number indicates that batteries with a negative polymer network can accept the current appropriately compared to line production batteries.

CONCLUSIONS

Reducing the weight of a vehicle is aimed in different ways, such as replacing heavy metal parts with well-engineered composites, high-quality polymers, and complicated alloys, by vehicle manufacturing companies. Lead-acid batteries are still very commonly used in different vehicles and reducing their weight could be another alternative to achieve this goal. This study revealed that the negative grid of the lead-acid batteries can be replaced with ABS without any reduction in its capacity. The results of measuring the capacity of a 30 amp 12-volt battery showed that this battery can generate capacity and a stable potential difference in the charging and discharging cycles. On the other hand, with the replacement of lead-coated polymer metals, significant weight loss has been created in the battery. An examination of the charging acceptance of a 30 amp 12-volt battery with a polymer grid shows that this battery successfully meets quality standards. The results of the start-up test in the cold showed that the battery with the polymer network has a lower quality of starter quality compared to the batteries of the production line, which goes back to the relatively low thickness of the conductor cover. In addition, the results of SEM showed that the thickness of the lead layer is about 13 μm, which makes the

Table 12. Charging results

Battery type	Current I_0	Battery charging current after 10 minutes (A)	Acceptance number
30 amps with lead network	3.3	9.43	2.8
30 amps with polymer/lead network	2.7	7.49	2.5

conductor conductive and stable in an acidic environment. A negative coated polymer network with lead network and generated capacity and discharge curve was investigated. The results show that the lead-coated polymer grid with a current of 0.5 amps per hour when discharged can create a stable potential difference in different cycles, but the capacity produced is less compared to the lead network. This is due to the active material falling from the surface of the plated polymer. Continuing from lead metal to due to its stability in acidic solution, it was used as the last layer of plating in the construction of expanding network. Direct connection of the lead flag using plastic injection may reduce the resistance of the battery and increase the capacity produced in the developed battery.

REFERENCES

1. J. Adams, M. Karulkar, *Power Sources*, 199 (2012).
2. H. Bode, *Lead-acid batteries*, John Wiley & Sons, United States (1977).
3. S. Gheytani, Y. Liang, F. Wu, Y. Jing, H. Dong, K. K. Rao, X. Chi, F. Fang and Y. Yao, *Adv. Sci*., **4**, 1700465 (2017).
4. A.Czerwiński, J. WrobelLach, K. Wrobel and P. Podsadni, *J. Solid State Electrochem*., **22**, 9 (2018).
5. J. Joseph, A. P. Mullane and K. Ostrikov, *ChemElectroChem*., 6 (2019).
6. D. Xu, L. Shen, F. Oqing, G. Kang, Y. Guan and Z. Peng, *J. Energy*, 218 (2021).
7. N. Javani, I. Dincer and G. F. Naterer, *J. Power Sources*, **5**, 268 (2014).
8. N. Javani, I. Dincer and G. F. Naterer, *J. Therm. Sci. Eng. Appl*., **7**(3), 031005 (2015).
9. S. M. He, J. Wang, X. Zhang, J. Chen, Z.Wang, T. Yang, Z. Liu, Y. Liang, B. Wang, S. Liu, L. Zhang, J. Huang, J. Huang, L. A. O'Dell and H. Yu, *Adv. Funct. Mater*., **29**, 1905228 (2019).
10. M. Angell, C. J. Pan, Y. Rong and H. Dai, *Proc. Natl. Acad. Sci*., 114 (2017).
11. S. Kumar, R. Satish, V. Verma, H. Ren, P. Kidkhunthodb, W. Manalastas Jr. and M. Srinivasan, *J. Power Sources*, 426 (2019).
12. D. Yuan and J. Zhao, *J. Manalastas, Sci*., **4**, 5 (2019).
13. Z. Hu, Y. Guo, H. Jin, H. Ji and L. A. Wan, *Chem. Commun*., 56 (2020).
14. J. AdamsKarulkar, *J. Power Sources*, 199 (2012).
15. E. B. Pinxterhuis, J. B. Gualtierotti, S. J. Wezenberg, J. G. Vries and B. L. Feringa, *ChemSus.Chem*., **11**, 1 (2018).
16. C. Li Z. Zhu, Y. Wang, Q. Guo, C. Wang, P. Zhong, Z. a. Tan and R. Yang, *Nano Energy*, 69 (2020).
17. D. Bathauer, *J. Renewable Energy Focus*., 16 (2015).
18. G. J. May, A. Davidson and B. Monahov, *J. Energy Storage*., **15**, 145 (2018).
19. A. J. Davidson, S. P. Binks and J. Gediga, *Int. J. Life Cycle Assess*., 21 (2016).
20. D. J. Moomaw, C. K. L. Mui and E. M. Hinojosa, US Patent, 10,693,141 (2020).
21. A. Czerwiński, J. Wrobel, J. Lach and K. WrobelPodsadni, *J. Solid State Electrochem*., 22 (2018).
22. Y. L. Gao, H. Guan, X. Fu, G. He, Y. Zhang, J. Wu and H. Wu, *Mater. Chem. Phys*., **257**, 123757 (2021).
23. J. Li, Y. Hu, Y. Zhang, J. Xie and P. K. Shen, *J. Electroanal. Chem*., 115065 (2021).
24. K. Varshney, P. K. Varshney, K. Gautam, M. Tanwar and M. Chaudhary, *Mater. Today Proceedings*, 26 (2020).
25. H. W. YehChang, C. J. Huang and G. G. Chen, *J. Electroanal. Chem*., **834**, 64 (2019).
26. S. y. Tan, D. J. Payne and J. P. HallettKelsall, *Curr. Opin. Electrochem*., **16**, 83 (2019).
27. C. Hu, J. Li, Q. Lan, T. Lan, J. Zhang, S. Zhou, Y. Rao, Y. Yanzhao and J. Cao, *Electrochim. Acta*, **384**, 138411 (2021).
28. M. Soria, J. Fullea, F. Saez and F. Trinidad, *J. Power Sources*, **78**, 220 (1999).
29. B. Culpin and K. Peters, *J. Power Sources*, **144**, 2 (2005).
30. A. Kirchev, N. Kircheva and M. Perrin, *J. Power Sources*, **19**, 620 (2011).
31. D. Egan, C. Low and F. Walsh, *J. Power Sources*, **196**, 13 (2011).
32. S. K. Martha, B. Hariprakash and S. A. Gaffoor, *J. Chem. Sci.*, **118**, 93 (2006).
33. S. Y. Lim, *J. Ind. Eng. Chem*., **78**, 284 (2019).
34. M. Asif, M. Rashad, J. H. Shah and S. D. A. Zaid, *J. Colloid Interface Sci*., **561**, 818 (2020).
35. N. Pinsky and S. A. Alkaitis, US Patent, 4,713,306 (1987).
36. S. Shivashankar, US Patent, 6,889,410 (2005).
37. Z. Hu, Y. Guo and H. Jin, *Chem. Commun*., **56**, 2023 (2020).
38. C. Wu, S. H. Gu and Q. H. Zhang, *Nat. Commun*., **10**, 1 (2019).
39. A. Liu, Z. Shi and R. G. Reddy, *Electrochim. Acta*, 251 (2017).
40. S. Pavlovic Zeidan, US Patent, 10,804,540 (2020).
41. V. Verma, S. Kumar and W. Manalastas, *Adv. Sustain. Syst*., **3**, 1800111 (2019).
42. W. He, A. Liu, J. Guan, Z. Shi, B. Gao and X. Hu, *RSC Adv*., **7**, 6902 (2017).
43. H. W. Yeh, Y. H. Tang and P. Y. Chen, *J. Electroanal. Chem*., **811**, 68 (2018).
44. J. C. Y. Jung, P. C. Sui and J. Zhang, *J. Energy Storage*., 35 (2021).
45. S. He, J. Wang, X. Zhang, J. Zhao, Z. Wang, T. Yang, Z. Liu, Y. Liang, B. Wang, S. Liu, L. Zhang, J. Huang and A. Huang, *J. Adv. Funct. Mater*., **29**, 45 (2019).